JACS
JOURNAL OF THE AMERICAN CHEMICAL SOCIETY

Communication

pubs.acs.org/JACS

Cooperative Thermodynamic Control of Selectivity in the Self-Assembly of Rare Earth Metal–Ligand Helices

Amber M. Johnson, Michael C. Young, Xing Zhang, Ryan R. Julian, and Richard J. Hooley*

Department of Chemistry, University of California—Riverside, Riverside, California 92521, United States

Supporting Information

ABSTRACT: Metal-selective self-assembly with rare-earth cations is possible with suitable rigid, symmetrical bis-tridentate ligands. Kinetically controlled formation is initially observed, with smaller cations preferentially incorporated. Over time, the more thermodynamically favorable complexes with larger metals are formed. This thermodynamic control is a cooperative supramolecular phenomenon and only occurs upon multiple-metal-based self-assembly: single-metal ML_3 analogues do not show reversible selectivity. The selectivity is dependent on small variations in lanthanide ionic radius and occurs despite identical coordination-ligand coordination geometries and minor size differences in the rare-earth metals.

The synthesis of supramolecular cage complexes through coordination chemistry is a rapidly expanding field. By combining metals (M) and ligands (L) with complementary geometry, many types of self-assembled structures can be designed and synthesized.[1] Three-dimensional cages are frequently targeted because their internal cavity can be exploited in host/guest chemistry, including stabilization of reactive species[2] and biomimetic catalysis.[3] With well-defined and predictable coordination geometries, *transition* metals are most often utilized in metal-mediated supramolecular self-assembly.[4]

Non-transition metals such as main-group and rare-earth (RE) metals have a number of advantages (such as oxidative stability and, in certain cases, diamagnetism) over transition metals in forming self-assembled systems, but the field of rare-earth-mediated self-assembly is far less explored. The roadblock is the variable coordination geometry displayed by lanthanide (Ln) metals, which makes predictable, controlled self-assembly rather challenging. By using tridentate chelating ligands, nine-coordinate complexes can be formed. Lanthanides have been used most often in the synthesis of M_2L_3 helices,[5] although tetrahedra[6] and other structures[7] have been reported. In these cases, the particular *type* of RE metal used in the self-assembly process is often overlooked: each RE is treated the same in terms of its assembly characteristics. Whereas transition metals display different coordination numbers and geometries, the coordination chemistry of the Ln series is relatively unchanged across the series. Each RE metal strongly favors the +3 oxidation state and commonly displays nine coordination sites. When attempting to *selectively* bind different REs, one can only exploit the Ln contraction and variations in effective ionic radius (EIR). The differences are not large: La^{3+} and Yb^{3+} are only separated by 0.2 Å in size, and adjacent REs are exceptionally similar in EIR. This makes selective binding and extraction of Ln metals (e.g., from spent nuclear waste streams) quite challenging.[8] Controlled, metal-selective self-assembly of RE M–L complexes would be applicable to both construction of functionalized cages and hosts and remediation of nuclear waste effluents. Here we describe the effect of self-assembly and cooperativity on the *selective* formation of self-assembled Ln helices based on a rigid, symmetrical bis-tridentate ligand.

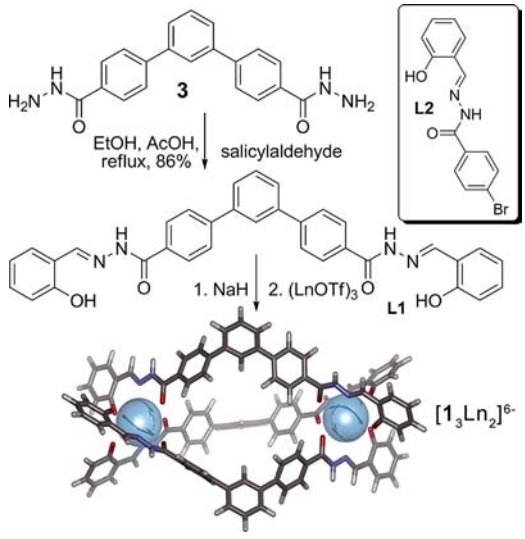

Figure 1. Synthesis of self-assembling ligand **L1**, control ligand **L2**, and bimetallic helices $[\mathbf{1}_3Ln_2]^{6-}$ (minimized structure, SPARTAN, AM1 force field).

The required tridentate coordination motif was provided by salicylhydrazone-based ligands (Figure 1). Bis-tridentate **L1** is capable of assembly with two metals into supramolecular aggregates, whereas **L2** acts as a control, capable of coordinating only a single metal. **L1** was synthesized by refluxing known[9] dihydrazide **3** with salicylaldehyde in ethanol and catalytic acetic acid. **L2** was synthesized from ethyl 4-bromobenzoate in two steps (see Supporting Information (SI)). In their neutral forms, neither **L1** nor **L2** showed any affinity for $Ln(OTf)_3$ salts in DMSO-d_6. Slight, very weak coordination was observed between **L1** and $Ln(OTf)_3$ salts in CD_3CN. To increase its coordinative capabilities, **L1** was exhaustively deprotonated by treatment with NaH. Tetraanionic **1** readily dissolved in DMSO-d_6 and displayed greatly enhanced coordinative properties. Simply

Received: September 24, 2013
Published: November 8, 2013

   dx.doi.org/10.1021/ja409882k | J. Am. Chem. Soc. 2013, 135, 17723–17726

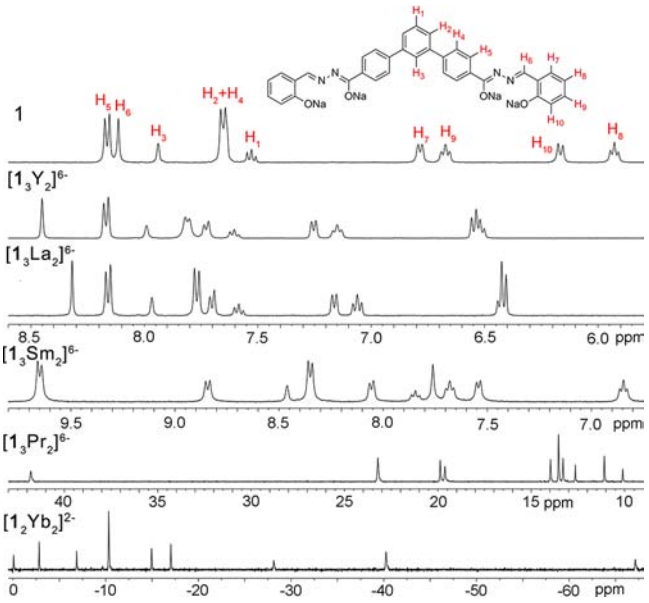

Figure 2. ^{1}H NMR spectra of self-assembled lanthanide helical complexes (400 MHz, DMSO-d_6).

titrating a DMSO solution of Sm(OTf)$_3$ into a solution of **1** assisted in determining the stoichiometry of the self-assembled complex. After addition of 0.67 mol equiv of metal, no peaks for ligand were observable by ^{1}H NMR, and a single, discrete M_2L_3 complex $[\mathbf{1}_3Sm_2]^{6-}$ was observed (see Figure 1 for a minimized structure).

The ligands can form self-assembled complexes with a range of RE metals. The chosen metals (La, Pr, Sm, Yb, and lanthanide surrogate Y) are spread across the Ln series and provide a range of ionic radii (Y is similar in size to Ho). Highly paramagnetic metals such as Gd and Dy were avoided to allow ^{1}H NMR analysis. Titration data were consistent for all the larger metals (La, Pr, Sm, Y) tested. The only deviation from the M_2L_3 stoichiometry was observed with the smaller REs such as Yb. When Yb(OTf)$_3$ was titrated into a solution of **1**, a full equivalent of metal was required for complete formation of complex, suggesting $[\mathbf{1}_2Yb_2]^{2-}$ is formed in this case. The titration data fit with the predicted structure of M_2L_x helices. Triple-stranded helices are formed with the larger metals, with nine coordination sites of the Ln being filled. The smaller Yb is less disposed to fit three tridentate ligands in its coordination sphere and instead forms a double-stranded M_2L_2 complex. Figure 2 shows the ^{1}H NMR spectra of the Ln complexes. Diamagnetic Y and La and weakly paramagnetic Sm appear as expected in the aromatic region, while paramagnetic Pr and Yb shift the complex resonances strongly downfield and upfield, respectively.

Further characterization was provided by diffusion NMR. DOSY spectra were taken for $[\mathbf{1}_3Y_2]^{6-}$ and $[\mathbf{1}_3Sm_2]^{6-}$ in DMSO-d_6. The observed diffusion coefficient for $[\mathbf{1}_3Y_2]^{6-}$ was 7.24×10^{-11} m^2/s, and that of $[\mathbf{1}_3Sm_2]^{6-}$ was 8.13×10^{-11} m^2/s, indicating that the two complexes display almost identical overall size and charge properties (for spectra see SI). No change in the ^{1}H NMR spectra was observed upon addition of different counteranions. Use of different LnX_3 salts (such as chloride or nitrate) also gave identical complexes, indicating that the Ln centers are saturated by **1**, with no interaction with the counterions.

While the complexes formed with **1** were only soluble in DMSO, treatment of **L1** with potassium *tert*-butoxide gave

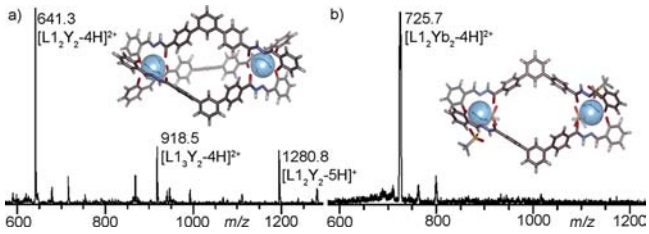

Figure 3. Mass spectra and minimized structures (SPARTAN, AM1 force field) of (a) $[\mathbf{1}_3Y_2]^{6-}$ and (b) $[\mathbf{1}_2Yb_2]^{2-}$.

complexes that were sufficiently soluble in THF for ESI-MS analysis. For each of the tested $[\mathbf{1}_3Ln_2]^{6-}$ assemblies, the parent $[M_2L_3\text{-}4H]^{2+}$ ions could be obtained under ESI analysis in positive mode. The acidic ionization conditions caused protonation of the complexes, and singly and doubly charged cations were observed. While the parent ion was observed in all cases, the species were susceptible to significant fragmentation. Loss of ligand was the most common fragmentation, and the $[M_2L_2\text{-}4H]^{2+}$ and $[M_2L_2\text{-}5H]^+$ ions were commonly observed. No higher stoichiometry (e.g., M_4L_6) aggregates were present, and the experimental isotope patterns agreed with the predicted M_2L_3 stoichiometry (see Figure 3 and SI). The $[\mathbf{L1}_3Ln_2\text{-}4H]^{2+}$ cation from $[\mathbf{1}_3Y_2]^{6-}$ and $[\mathbf{1}_3Sm_2]^{6-}$ was subjected to MS/MS analysis, resulting in fragmentation to the singly and doubly charged M_2L_2 cations. This suggests that the M_2L_2 complexes observed are a result of ligand loss under ionizing conditions and not from incomplete assembly. Analysis of $[\mathbf{1}_2Yb_2]^{2-}$ gave no ions arising from the M_2L_3 complex, consistent with its NMR assignment. Despite extensive experimentation, single crystals of the complexes could not be obtained. The charged species in DMSO solution were susceptible to protonation with adventitious water, and crystallization from less favorable solvents such as THF complexes led to metal extrusion.

While each of the tested REs was capable of forming self-assembled helices, the ligand showed significant selectivity between differently sized metals. Two types of experiments were performed to illustrate the selectivity: initial kinetic preference via a displacement test and thermodynamic preference after equilibration. The initial kinetic selectivity was tested by titrating a DMSO-d_6 solution of $Ln^A(OTf)_3$ into a solution of preformed $[\mathbf{1}_3Ln^B{}_2]^{6-}$ and determining the extent of displacement of the first metal by the second from ^{1}H NMR integration. This displacement assay showed a clear correlation between EIR of the metal and the preference for displacement, with smaller radius cations being favored (for full spectra and tabulation, see SI). Almost complete displacement of La^{3+} was observed upon titrating 0.67 mol equiv of Y(OTf)$_3$ (EIR = 1.02 Å) to $[\mathbf{1}_3La_2]^{6-}$ (see SI). When La(OTf)$_3$ (EIR = 1.18 Å) was added to $[\mathbf{1}_3Y_2]^{6-}$, no displacement was observed. Interestingly, no heterometallic $[\mathbf{1}_3YLa]^{6-}$ was observed in this case. With other metal combinations that had smaller variance in EIR, lower overall selectivity and the presence of heterometallic complexes were observed. While overlapping signals plagued the analysis of heterometallic complexes of two diamagnetic metals (Y, La, Sm), paramagnetic Pr^{3+} and Yb^{3+} acted as shift reagents, separating the signals and aiding identification. Figure 4 shows the corresponding NMR spectra, as well as the selectivity and EIR data.

To determine whether this kinetic selectivity was a supramolecular effect or merely a characteristic of the coordinating ligand, control experiments were performed with **2**. When 0.33 mol equiv of Ln(OTf$_3$) was added to a DMSO-d_6 solution of **2**, a clean ML_3 complex $[\mathbf{2}_3Ln]^{3-}$ was formed. ESI-MS analysis

dx.doi.org/10.1021/ja409882k | J. Am. Chem. Soc. 2013, 135, 17723−17726

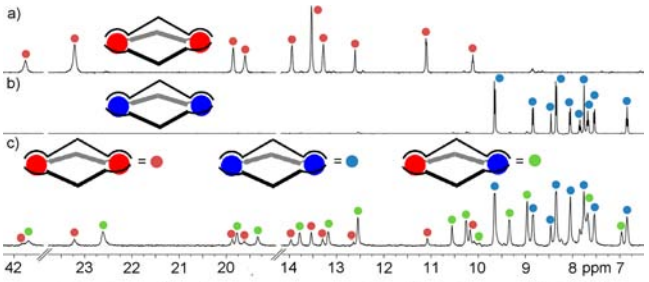

Metals	%A_2	%B_2	%AB	Ln^{3+}	EIR (Å)[10]
Y:La	97	3	0	La	1.18
Y:Pr	70	15	15	Pr	1.14
Y:Yb	5	55	40	Sm	1.09
La:Sm	10	57	33	Y	1.02
Pr:Sm	7	57	36	Yb	0.98

Figure 4. Identification of heterometallic complexes: (a) $[\mathbf{1}_3Pr_2]^{6-}$; (b) $[\mathbf{1}_3Sm_2]^{6-}$; and (c) mixture of $[\mathbf{1}_3Pr_2]^{6-}$ (red), $[\mathbf{1}_3Sm_2]^{6-}$ (blue), and $[\mathbf{1}_3PrSm]^{6-}$ (green). Below: percentage of complexes after displacement titrations and effective ionic radii of Ln^{3+} ions.

showed the presence of the $[Ln\mathbf{L2}_3\text{-}2H]^+$ parent ion, along with fragmentation into the $[Ln\mathbf{L2}_2\text{-}2H]^+$ ion, analogous to that observed with **1**. MS/MS analysis of the $[Ln\mathbf{L2}_3\text{-}2H]^+$ parent ion showed fragmentation of the ML_3 complex into the $[Ln\mathbf{L2}_2\text{-}2H]^+$ ion. The monometal $[\mathbf{2}_3Ln]^{3-}$ complexes showed the same kinetic preference for metals with smaller ionic radii as the bimetallic helices $[\mathbf{1}_3Ln_2]^{6-}$ according to displacement experiments. The relationship between the difference in EIR of the added metals and the observed concentration of $[\mathbf{1}_3Ln(small)_2]^{6-}$ upon displacement showed a strongly linear correlation (see SI). As Δ(EIR) increased, so did the selectivity for the smaller metal. The kinetic selectivity for smaller metals is evidently a charge-based phenomenon. As the metal EIR decreases, the charge:size ratio increases, as does the affinity of the anionic ligand for the smaller metal.

While these displacement experiments described the *kinetic* preference of the Ln–L complexes, far more unusual behavior was observed upon equilibration of the self-assembled Ln helices. To test equilibration, an equimolar mixture of metals was added to a solution of **1**, and ^1H NMR spectra were periodically acquired over 30 h. Figure 5 shows the percentage of each complex (both homometallic $[\mathbf{1}_3Ln^A{}_2]^{6-}$ and $[\mathbf{1}_3Ln^B{}_2]^{6-}$, and heterometallic $[\mathbf{1}_3Ln^ALn^B]^{6-}$) vs time with mixtures of Y^{3+}, La^{3+}, and Sm^{3+} (for complete analysis see SI). In all samples, the initially formed kinetic complex was that favored in the displacement experiments; i.e., the smaller cation was preferentially bound. Over time, the selection preference inverted: for the highly selective Y/La mixture, the kinetically disfavored $[\mathbf{1}_3La_2]^{6-}$ was observed after 3 h equilibration. Equilibration was complete after 24 h, and only the larger $[\mathbf{1}_3La_2]^{6-}$ complex was present. The selectivity of self-assembly after equilibration again depended on Δ(EIR) of the cations, but the thermodynamically favored complexes are formed with the *larger* metal. The Y^{3+}/La^{3+} mixture (Figure 5a) displays the largest Δ(EIR), and the initial 96:4:0 ratio of $[\mathbf{1}_3Y_2]^{6-}$:$[\mathbf{1}_3La_2]^{6-}$:$[\mathbf{1}_3LaY]^{6-}$ complexes was inverted to 6:94:0 after equilibration, preferentially forming the larger $[\mathbf{1}_3La_2]^{6-}$ complex. In the Y^{3+}/Sm^{3+} mixture (Figure 5b), with a smaller Δ(EIR), the initial ratio was 50:9:4, and after equilibration it was 17:37:46. The selection process after equilibration also showed a direct, linear dependence on Δ(EIR) (for graphs, see SI). Whereas the initial selectivity favored smaller metal binding, the thermodynamic product was that of the larger metal complex. As Δ(EIR) increased, the thermodynamic favorability for incorporation of the larger metal increased. The ligand was again strongly selective for the Y/La combination, which displays a Δ(EIR) between the metals of only 0.16 Å. Smaller Δ(EIR) led to observation of heterometallic complexes, and the concentration of $[\mathbf{1}_3Ln^ALn^B]^{6-}$ was also dependent on Δ(EIR), with a greater size difference resulting in a smaller proportion of heterometallic complex. The observed selectivity with our rigid anionic coordinators is much greater than that observed with flexible, neutral bis-tridentate Ln chelators.[11] In that case, very similar proportions of $(Ln^A)_2$, $(Ln^B)_2$, and (Ln^{AB}) complexes were formed upon addition of equimolar amounts of different metals.[11]

The inverted selectivity upon equilibration phenomenon is truly a supramolecular effect and requires a self-assembling ligand to occur. When ML_3 complexes were formed from monometallic control ligand **2**, essentially *no* equilibration was observed, even after extensive periods of time. In this case, *both* the kinetic and thermodynamic preferences for metal complexation are determined by the electronic coordination properties of the ligand alone. This favors small metals with a larger charge:size ratio (see Figure 5d–f).

The presence of the second coordination site in a rigid ligand such as **1** adds another dimension to the selectivity of self-assembly. Coulombic interactions are no longer the sole determining factor in coordination: the added strain upon the rigid coordinating ligand must be considered. The flexible

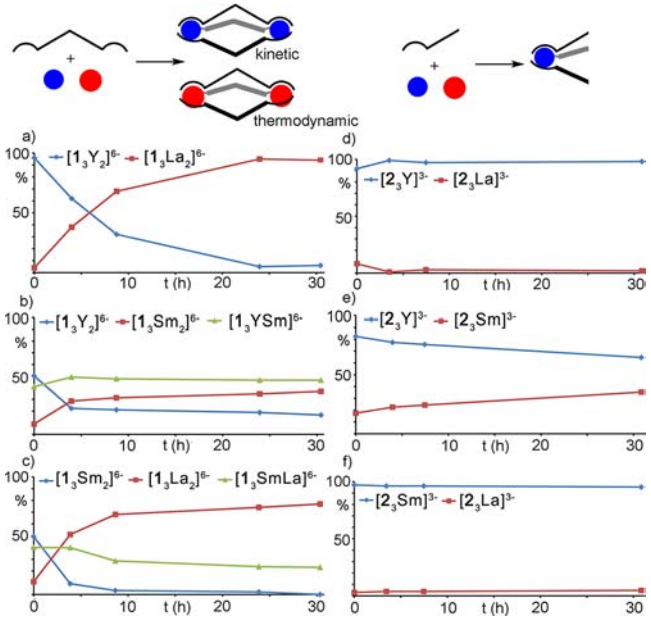

Figure 5. Equilibration of lanthanide complexes: (a) $\mathbf{1}_3Y_2$ vs $\mathbf{1}_3La_2$; (b) $\mathbf{1}_3Y_2$ vs $\mathbf{1}_3Sm_2$; (c) $\mathbf{1}_3Sm_2$ vs $\mathbf{1}_3La_2$; (d) $\mathbf{2}_3Y$ vs $\mathbf{2}_3La$; (e) $\mathbf{2}_3Y$ vs $\mathbf{2}_3Sm$; and (f) $\mathbf{2}_3Sm$ vs $\mathbf{2}_3La$ (DMSO-d_6, 298 K).

coordination sphere of RE metals allows ligands to shift into more favorable conformations around the metal to minimize strain and steric congestion between ligands.[12] In the $[\mathbf{1}_3La_2]^{6-}$ complexes, the two coordination sites are connected by rigid aromatic rings, restricting conformational flexibility and adding strain to the complex. Larger metals provide more space for a favorable conformation to be reached and so are preferentially coordinated, if equilibration can be reached. The use of rigid,

dx.doi.org/10.1021/ja409882k | J. Am. Chem. Soc. 2013, 135, 17723–17726

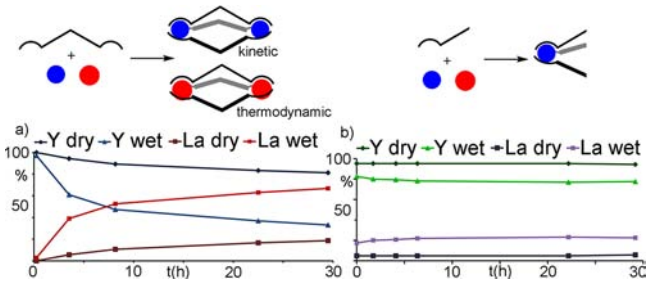

Figure 6. Plots of percent complex vs time: (a) $[\mathbf{1}_3Y_2]^{6-}$ and $[\mathbf{1}_3La_2]^{6-}$ in samples containing 50 mM water (dry) and 150 mM water (wet); (b) $\mathbf{2}_3Y$ and $\mathbf{2}_3La$ in samples containing 100 mM water (dry) and 300 mM water (wet).

strained ligands to control assembly in *transition metal* complexes is precedented,[1,13] but it is rarely observed for coordinatively flexible RE metal complexes. **1** is a departure from the more typical Ln-coordinating ligands that contain flexible methylene spacers and show little to no selectivity between metals unless "built in" by the incorporation of different coordinating motifs.[14]

Interestingly, the presence of water in the sample has a large effect on the equilibration process. Water is well-known to reversibly coordinate to Gd-based MRI contrast agents and is strongly correlated with their contrast and relaxivity.[15] For the $[\mathbf{1}_3La_2]^{6-}$ complexes, increased $[H_2O]$ caused faster equilibration to the thermodynamic product. The data are most striking for the Y^{3+}/La^{3+} system: Figure 6 shows the change in proportion of $[\mathbf{1}_3Y_2]^{6-}$ and $[\mathbf{1}_3La_2]^{6-}$ vs time, along with the control of $[\mathbf{2}_3Y]^{3-}$: $[\mathbf{2}_3La]^{3-}$ in samples containing varying amounts of water. In the presence of 50 mM water, very slow equilibration of $[\mathbf{1}_3Y_2]^{6-}$ to $[\mathbf{1}_3La_2]^{6-}$ occurs and the equilibration is not complete after multiple days. Additional water ($[H_2O]$ = 150 mM) caused a much faster change in the equilibrium, and the graph is similar to Figure 5a. It should be noted that $[H_2O]$ in all equilibration experiments in Figure 5 and the SI was identical.

As would be expected, monometallic control complex $[\mathbf{2}_3Y]^{3-}$ showed no effect from the presence of additional water. There was a slight shift in selectivity upon initial complexation, but no significant equilibration was observed, lending additional evidence for cooperativity in equilibration. The favorable, reversible coordination of water to the Ln centers allows more rapid on/off exchange between the ligands and speeds up the equilibration process. In the case of the nonequilibrating ligand **2**, this has essentially no effect but is an important component of the cooperative selectivity of **1** for different RE metals.

In conclusion, we have shown that self-assembled M_2L_3 complexes can discriminate among lanthanide ions with a kinetic preference for smaller metals and a thermodynamic preference for larger metals. Selectivity is obtained despite small differences in Ln ion size and identical coordination environment of the ligand, and a correlation is observed between distribution of complex and difference in ionic radius. Cooperative effects are observed in the bis-tridentate ligand, and the presence of two coordination sites assists in equilibration to the larger complex. Further studies of lanthanide- and actinide-based self-assembly are underway in our laboratory.

■ ASSOCIATED CONTENT

Ⓢ Supporting Information

Experimental details and characterization data. This material is available free of charge via the Internet at http://pubs.acs.org.

■ AUTHOR INFORMATION

Corresponding Author

richard.hooley@ucr.edu

Notes

The authors declare no competing financial interest.

■ ACKNOWLEDGMENTS

The authors thank the NSF (CHE-1151773 to R.J.H., CHE-0747481 to R.R.J.) and UC Riverside for funding.

■ REFERENCES

(1) Fujita, M.; Umemoto, K.; Yoshizawa, M.; Fujita, N.; Kusukawa, T.; Biradha, K. *Chem. Commun.* **2001**, 509.

(2) Fiedler, D.; Bergman, R. G.; Raymond, K. N. *Angew. Chem., Int. Ed.* **2006**, *45*, 745.

(3) Brown, C. J.; Bergman, R. G.; Raymond, K. N. *J. Am. Chem. Soc.* **2009**, *131*, 17530.

(4) Young, N. J.; Hay, B. P. *Chem. Commun.* **2013**, *49*, 1354.

(5) (a) Piguet, C.; Bernardinelli, G.; Hopfgartners, G. *Chem. Rev.* **1997**, *97*, 2005. (b) Stomeo, F.; Lincheneau, C.; Leonard, J. P.; O'Brien, J. E.; Peacock, R. D.; McCoy, C. P.; Gunnlaugsson, T. *J. Am. Chem. Soc.* **2009**, *131*, 9636. (c) Shi, J.; Hou, Y.; Chu, W.; Shi, X.; Gu, H.; Wang, B.; Sun, Z. *Inorg. Chem.* **2013**, *52*, 5013. (d) Jensen, T. B.; Scopelliti, R.; Bünzli, J.-C. G. *Chem.—Eur. J.* **2007**, *13*, 8404. (e) Piguet, C.; Bünzli, J.-C. G. In *Handbook on the Physics and Chemistry of Rare Earths*; Gschneider, K. A., Jr., Bünzli, J.-C. G., Pecharsky, V. K., Eds.; Elsevier: Amsterdam, 2010; Vol. *40*, pp 301−553. (f) Albrecht, M.; Osetska, O.; Frölich, R.; Bünzli, J.-C. G.; Aebischer, A.; Gumy, F.; Hamacek, J. *J. Am. Chem. Soc.* **2007**, *129*, 14178. (g) Ryan, P. E.; Guénée, L.; Piguet, C. *Dalton Trans.* **2013**, *42*, 11047.

(6) (a) Wang, J.; He, C.; Wu, P.; Wang, J.; Duan, C. *J. Am. Chem. Soc.* **2011**, *133*, 12402. (b) El Aroussi, B.; Guénée, L.; Pal, P.; Hamacek, J. *Inorg. Chem.* **2011**, *50*, 8588.

(7) (a) Chen, X.-Y.; Bretonnière, Y.; Pécaut, J.; Imbert, D.; Bünzli, J.-C.; Mazzanti, M. *Inorg. Chem.* **2007**, *46*, 625. (b) El Aroussi, B.; Zebret, S.; Besnard, C.; Perrottet, P.; Hamacek, J. *J. Am. Chem. Soc.* **2011**, *133*, 10764.

(8) (a) Gorden, A. E. V.; DeVore, M. A., II; Maynard, B. A. *Inorg. Chem.* **2013**, *52*, 3445. (b) Lewis, F. W.; Hudson, M. J.; Harwood, L. M. *Synlett* **2011**, *18*, 2609. (c) Paiva, A. P.; Malik, P. *J. Radioanal. Nucl. Chem.* **2004**, *261*, 485. (d) Panak, P. J.; Geist, A. *Chem. Rev.* **2013**, *113*, 1199.

(9) Johnson, A. M.; Young, M. C.; Hooley, R. J. *Dalton Trans.* **2013**, *42*, 8394.

(10) *CRC Handbook of Chemistry and Physics*, 87th ed.; Lide, D. R., Ed.; CRC Press: Boca Raton, FL, 2006; Sect. 4, p 132.

(11) Piguet, C.; Bünzli, J.-C. G.; Bernardinelli, G.; Hopfgartner, G.; Williams, A. F. *J. Am. Chem. Soc.* **1993**, *115*, 8197.

(12) (a) Petoud, S.; Bünzli, J.-C. G.; Renaud, F.; Piguet, C.; Schenk, K. J.; Hopfgartner, G. *Inorg. Chem.* **1997**, *36*, 5750. (b) Le Borgne, T.; Bénech, J.-M.; Floquet, S.; Bernardinelli, G.; Aliprandini, C.; Bettens, P.; Piguet, C. *Dalton Trans.* **2003**, 3856.

(13) (a) Young, M. C.; Johnson, A. M.; Gamboa, A. S.; Hooley, R. J. *Chem. Commun.* **2013**, *49*, 1627. (b) Ousaka, N.; Grunder, S.; Castilla, A. M.; Whalley, A. C.; Stoddart, J. F.; Nitschke, J. R. *J. Am. Chem. Soc.* **2012**, *134*, 11528.

(14) (a) Sorgho-Aboshyan, L.; Nozary, H.; Aebischer, A.; Bünzli, J.-C. G.; Morgantini, P.-Y.; Kittilstved, K. R. *J. Am. Chem. Soc.* **2012**, *134*, 12675. (b) Albrecht, M.; Osetska, O.; Bünzli, J.-C. G.; Gumy, F.; Fröhlich, R. *Chem.—Eur. J.* **2009**, *15*, 8791. (c) Zeckert, K.; Hamacek, J.; Rivera, J.-P.; Floquet, S.; Pinto, A.; Borkovec, M.; Piguet, C. *J. Am. Chem. Soc.* **2004**, *126*, 11589. (d) Riis-Johannessen, T.; Bernardinelli, G.; Filinchuk, Y.; Clifford, S.; Favera, N. D.; Piguet, C. *Inorg. Chem.* **2009**, *48*, 5512.

(15) Caravan, P.; Ellison, J. J.; McMurry, T. J.; Lauffer, R. B. *Chem. Rev.* **1999**, *99*, 2293.